PREPRINT UCRL-77116

CONF-750836--1

Lawrence Livermore Laboratory

THREE-DIMENSIONAL STRESS DISTRIBUTION

OF A DOUBLE-CANTILEVER BEAM WITH A SIDE NOTCH

W.F. Kirkwood
M.E. Prado

August 8, 1975

This paper was prepared for submission to the 9th National Symposium on Fracture Mechanics sponsored by American Society for Testing and Materials, Committee E-24 on Fracture Testing of Metals, Pittsburgh, PA, August 25-27, 1975

THREE-DIMENSIONAL STRESS DISTRIBUTION OF A DOUBLE-CANTILEVER BEAM WITH A SIDE NOTCH*

W.F. Kirkwood and M.E. Prado

Lawrence Livermore Laboratory, University of California

Livermore, California 94550

ABSTRACT

The effect of a side notch used as a crack guide in a double-cantilever-beam specimen is investigated. The resulting stress distribution along the section of symmetry ahead of the notch is obtained from a three-dimensional photoelastic model. The effect of the side notch, through the thickness and down the side of the specimen is determined. After stress freezing, the model was sliced along principal planes. Along the x-x plane of symmetry, the principal stresses were determined by graphical integration of Filon's transformation of the Lame'-Maxwell equations and by subslicing along the x-z plane. Results of the investigation are in good agreement with those of other investigators. The side notch increases the value of the maximum tensile stress at the intersection of the starter notch and the side notch by approximately 22%.

*This work was performed under the auspices of the U.S. Energy Research & Development Administration.

KEY WORDS

Double cantilever beam, side notch, stress freezing, starter notch, stress-intensity factor, fringes, photoelasticity, fracture, stress fringes

NOMENCLATURE

a	Distance from loading pin center line to notch tip (mm)
B	Minimum through-the-thickness distance between side notches (mm)
d	Distance from the notch tip to the end of the specimen (mm)
P	Load (N)
R_N	Notch root radius (mm)
W	Distance from loading pin center line to the end of the specimen (mm)
K_I	Stress intensity factor for Mode I type of displacement [$MPa \cdot m^{1/2}$]
$\sigma_x, \sigma_y, \sigma_z$	Cartesian system stress components
n	Fringe order
f	Material fringe value (N/mm per fringe)
t	Thickness of the model slice (mm)
σ_n	Nominal combined bending and tensile stresses (Pa)

INTRODUCTION

Experimental work in determining stress-intensity factors and three-dimensional effects has been conducted on compact specimens. Schroedl and Smith [1] have performed analysis on compact specimens for W/B and a/W ratios as recommended in ASTM E-399. However, although other geometries are often used to characterize material toughness, the effort to determine the three-dimensional effects on the stress intensity of other geometries has not been made to the same degree as in the case of compact specimens. Specifically, the use of the side notch in the double-cantilever beam (DCB) has not been explored to determine the effect of the notch on the through-thickness stress intensity-factor. Mostovoy [2] presents the general approach for the use of this class of specimens, and Gallagher [3] and Dull [4] discuss the determination of experimentally determined stress intensity factors and the compliance calibration for these specimens. The use of the contoured double cantilever beam specimen is for determining fatigue properties, material stress-corrosion resistance, and fracture toughness. Because of the geometric advantage which the DCB specimen offers, a program for determining the fracture toughness of beryllium was initiated in 1970 at Lawrence Livermore Laboratory (LLL) using DCB specimens [5]. This work served to motivate the present study. The DCB specimens used in Ref. 5 were side notched but no attempt was made to determine the influence of a side notch on fracture toughness. The present study is thus aimed at evaluating side-notched specimens with the goal of determining their three-dimensional stress distribution.

This study is restricted to one-notched geometry with a specific crack length. However, a thorough experimental stress analysis of this geometry has been made and it is believed that the conclusions reached in this study should be relevant to other side-notched geometries.

EXPERIMENTAL PROCEDURE

The photoelastic specimens employed in these experiments are machined from readily available epoxy resins which exhibit excellent characteristics for use in three-dimensional models. Leven [6] has detailed the techniques and procedures for successfully employing phthalic-anhydride cured resins and the authors have had good results with these materials. After casting and fabrication, the model is placed in an oven and loaded with dead weights. The oven is slowly heated to 165°C, which is the desired "stress freezing" [7] temperature for this material, and then slowly cooled to ambient temperature. At this point the stresses are permanently locked into the specimen and it is ready for slicing and analysis.

MODEL SLICING AND FRINGE EVALUATION

Figure 1 shows the coordinate system employed in this investigation. The specimen geometry is described in Fig. 2 and the slicing plan is shown in Fig. 3. Figure 4 shows the stress patterns in the center slice $\left(\frac{2z}{B} = 0\right)$. These patterns are similar at $\frac{2z}{B} = 0.4$ and 0.6. The numbers in the field of these photographs refer to fringe order (n). Figure 5 is a slice taken at

the edge of the specimen and includes the side notch. Figure 6 shows stress patterns of two slices removed tangent to the starter notch for determining the fringe orders along the Z axis. By determining the fringe order at an initial slice thickness and determining $\frac{n}{t}$ through a series of machining operations, the final values of the stress differences $\sigma_y - \sigma_z$ may be extrapolated to the free boundary along the starter notch.

From the stress patterns shown in Figs. 4 and 5, the principal stresses in the region of the starter notch were determined and are plotted in dimensionless form in Fig. 7. Separation of the principal stresses was accomplished using the slope equilibrium method [7], Filon's transformation of the Lame-Maxwell equations [8] and by sub-slicing. The determination of fractional fringe orders was accomplished using Tardy Compensation [9], a Babinet compensator and by extrapolation to a boundary.

DISCUSSION OF EXPERIMENTAL ANALYSIS AND RESULTS

Figure 4 shows a light field photograph of a slice removed from the center or mid-thickness of the model. Along the X axis, the fringe pattern (see numbers on field of photograph) ranges from an order of zero at the isotropic point to a maximum of 5.6 at the root radius. Along this principal axis σ_x and σ_y are principal stresses. In each case the stress pattern was analyzed by applying the stress optic law [8]

$$\sigma_x - \sigma_y = \frac{nf}{t} . \qquad (1)$$

The determination of the principal stresses through the thickness (along the Z axis at the root of the notch) is handled in the same manner with

$$\sigma_y - \sigma_z = \frac{nf}{t} \quad . \tag{2}$$

The general form for the elastic-stress field near a crack tip of zero root radius by Irwin [10] is

$$\sigma_y = \frac{K_I}{(2\pi r)^{1/2}} \cos\frac{\theta}{2}\left(1 + \sin\frac{\theta}{2}\sin\frac{3\theta}{2}\right) . \tag{3}$$

As our model has a small finite root radius, it does not satisfy Eq. (3) because r never approaches zero. Bowie and Neal [11] performed investigations employing finite root radius with results showing that for a notch-length-to-root-radius ratio greater than 2.0, there is introduced a maximum 2% error in determining K_I. Kobayashi [12] determined through a series of photoelastic experiments that K_I reaches a stationary value when the minimum value of r is approximately 1.85 mm. The boundary stresses σ_y/σ_n determined at the notch root through the thickness from 2Z/B = 0 to 0.75 varies approximately 3-1/2%, which is an acceptable span for experimental error. Therefore, it will be assumed for this investigation that equation (3) provides values within 6% near the starter notch root.

The stress intensity factors were determined using the dimensionless form suggested by Marloff et al. [13] in which

$$\sigma_n = \frac{P}{Bd}\left(4 + \frac{6a}{d}\right) . \tag{4}$$

Setting $\theta = 0$ in equation (3)

$$K_I = (2\pi r)^{1/2}\,\sigma_y \tag{5}$$

By setting r = x and dividing numerator and denominator by $d^{1/2}$, a convenient equation for both stress analysis and plotting may be developed:

$$K_I = (2\pi d)^{1/2} \left(\frac{x}{d}\right)^{1/2} \sigma_y \ . \qquad (6)$$

By substituting $(a)^{1/2}/\sigma_n$ into both sides of equation (6), the stress intensity factor may be expressed in dimensionless form:

$$\frac{K_I (a)^{1/2} B}{P} = 7.97 \left(\frac{x}{d}\right)^{1/2} \left(\frac{\sigma_y}{\sigma_n}\right). \qquad (7)$$

Figures 8 and 9 show the stress distribution along the Z axis from the center of the specimen out to the side notch. For most of this distance it behaves as though it doesn't know the side notch is there, but the discontinuity slowly influences it and by $2Z/B = 0.97$, a minimum value is reached with the σ_y/σ_n stress rapidly increasing to the side notch. So for a value of R_N = 0.51 mm with a 30° flank angle, the side notch influences the distribution of principal stresses for a distance of approximately 1.3 times the side notch radius. The effects of the side notch may be beneficial in maintaining a more even stress distribution through the specimen thickness and ensuring a more uniform crack length through the thickness.

The values of σ_z/σ_n were higher than anticipated but this is probably due to the high Poisson's ratio of the model material (0.48) at the stress-freezing temperature. Also the triaxial state of stress near the notch tip indicates that the condition of plane strain exists. Figure 8 shows the principal stresses in the X-Y plane at the center and along the side notch of the specimen. Starting at the notch root and going along the X axis, the values of σ_y/σ_n are always higher along the side notch compared to the center, a condition which should be expected at a free boundary and probably guarantees good crack guidance.

Figure 10 is a plot of the stress intensity factors near the starter notch. These plots were made for values of x/d between 0.001 to 0.015. It appears that these values become constant beyond x/d = 0.007.

CONCLUSIONS

The results of this investigation indicate that the use of a side notch in symmetrical fracture-toughness specimens provides the crack the guidance for which it was intended. Furthermore, the side notch, although it acts as a stress riser, tends to raise the average boundary stress from the region z/B = 0.75-1.00 to nearly the same as the mid-thickness value and will guarantee a more constant crack length throughout the complete thickness.

ACKNOWLEDGMENT

The authors wish to acknowledge the contribution of Mr. J.C. Stone for his skill in machining, testing and photographing the model.

REFERENCES

[1] Schroedl, M.A. and Smith, C.W., "Influences of Three-Dimensional Effects on the Stress Intensity Factors of Compact Specimens," in Fracture Analysis (ASTM Special Technical Publication 560, American Society for Testing and Materials, Philadelphia, 1974), pp. 69-80.

[2] Mostovoy, S., Crosley, P.B., and Ripling, E.J., J. Mater. 2, 661 (1967).

[3] Gallagher, J.P., Eng. Fract. Mech. 3, 1 (1971), pp. 27-43.

[4] Dull, D.L., Buch, J.D., and Raymond, L., Eng. Fract. Mech. 4, (1972), pp. 523-531.

[5] Prado, M.E., "Evaluation of Fracture Toughness of Beryllium," Lawrence Livermore Laboratory, Rept. UCID-15970, Rev. 1, (1979).

[6] Leven, M.M., "Epoxy Resins for Photoelastic Use," in Proc. Int. Sympos. on Photoelasticity, Chicago, 1961 (the MacMillan Co., New York, 1963).

[7] Hetenyi, M., Handbook of Experimental Stress Analysis (John Wiley & Sons, New York, 1950), pp. 933-936.

[8] Frocht, M.M., Photoelasticity (John Wiley & Sons, New York, 1941), Chapter 1.

[9] Gorasen, R.W. and Adams, L.H., J. Franklin Inst. 216, 4 (1933), pp. 475-504.

[10] Irwin, G.R. Kies, J.A., and Smith, H.L., Proc. ASTM 58 (1958), pp. 640-657.

[11] Bowie, O.L. and Neal, D.M., Int. J. Fract. Mech. 3, 2 (1967), pp. 111-119.

[12] Kobayashi, A.S., "Photoelastic Studies of Fracture," in Handbook of Fracture, Vol. 3 (Academic Press, New York, 1971), pp. 311-369.

[13] Marloff, R.H., Leven, M.M., Ringler, T.N., and Johnson, R.L., Exper. Mech. 11, 12 (1971), pp. 529-539.

FIGURE CAPTIONS

Fig. 1 Coordinate system for the stress field near the crack tip. The Z axis is perpendicular to the page.

Fig. 2 Dimensions of photoelastic model.

Fig. 3 Specimen-slicing plan.

Fig. 4 Light-field photographs of center slice and enlargement of stress pattern at crack tip. Slice is at 0.89 mm thickness. Notch-tip enlargement is 20×. Numbers in field refer to fringe order (n).

Fig. 5 Light-field photographs of edge slice, showing side notch. Top section is 4.11 mm thick. Lower left section showing crack tip (20×) is 0.41 mm thick. Lower right section showing crack tip (20×) is 0.41 mm thick. The thinning of the sections was used in: (a) determination of values of $\sigma_y - \sigma_z$ down the side notch axis and (b) determining maximum values of σ_y at the intersection of the crack tip and the notch. Numbers in field refer to fringe order (n).

Fig. 6 Stress pattern looking along trace of starter notch out to the side notch along the z-z plane. Upper slice thickness = 0.58 mm (20×). Lower slice thickness = 0.21 (20×).

Fig. 7 Distribution of the principal stresses (σ_y/σ_n and σ_z/σ_n) through the thickness at the notch tip.

Fig. 8 Through-the-thickness variations of the principal stresses along the z-z axis.

Fig. 9 Through-the-thickness variation of the maximum starter-notch stresses near the side notch.

Fig. 10 Plot of stress-intensity factors at center section and at side notch.

IMM/md

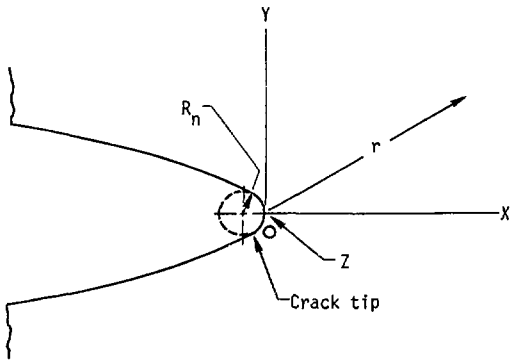

Kirkwood - Fig. 1

Notes:

1. All dimensions in mm
2. Starter notch and side notch have same radius

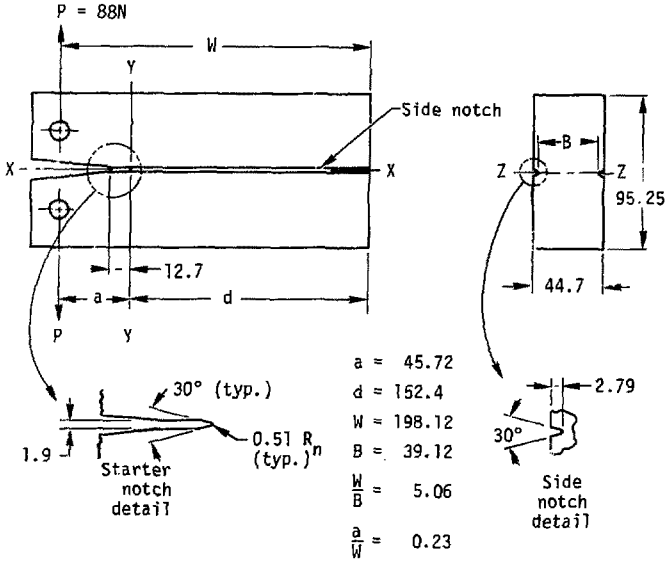

$a = 45.72$

$d = 152.4$

$W = 198.12$

$B = 39.12$

$\frac{W}{B} = 5.06$

$\frac{a}{W} = 0.23$

Kirkwood - Fig. 2

F2

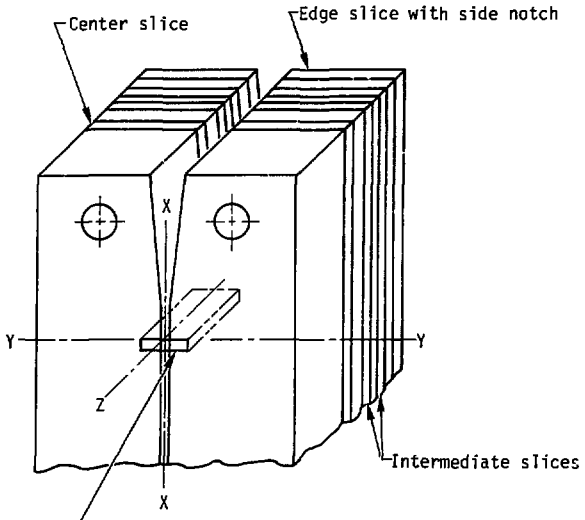

Slice tangent to starter notch root taken to determine $\sigma_y - \sigma_z$ at the root. Values we e extropolated to the free boundary by thinning several times and recording the fringe values.

Kirkwood - Fig. 3

F3

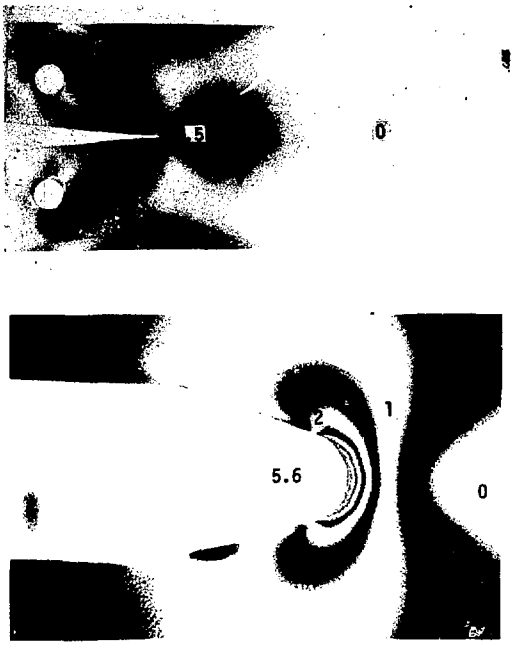

Kirkwood - Fig. 4

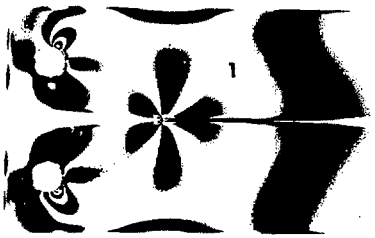

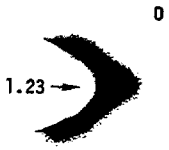

Kirkwood - Fig. 5

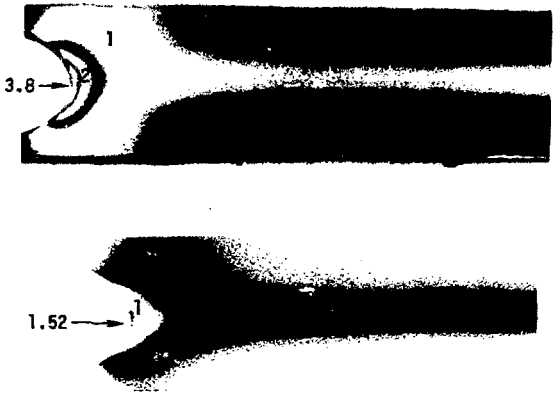

Kirkwood - Fig. 6

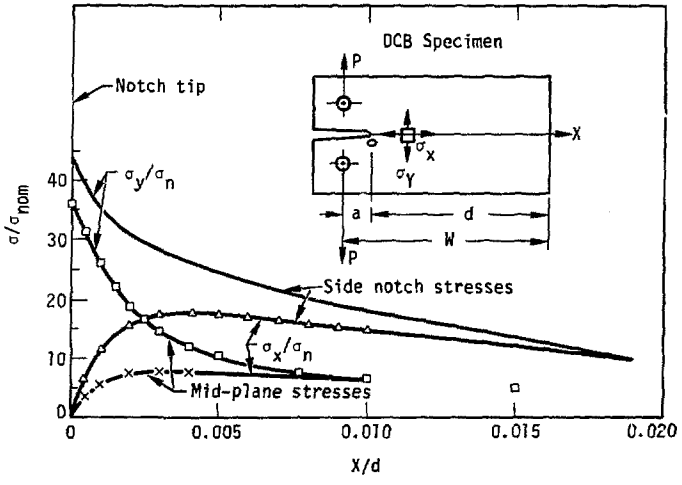

Kirkwood - Fig. 7

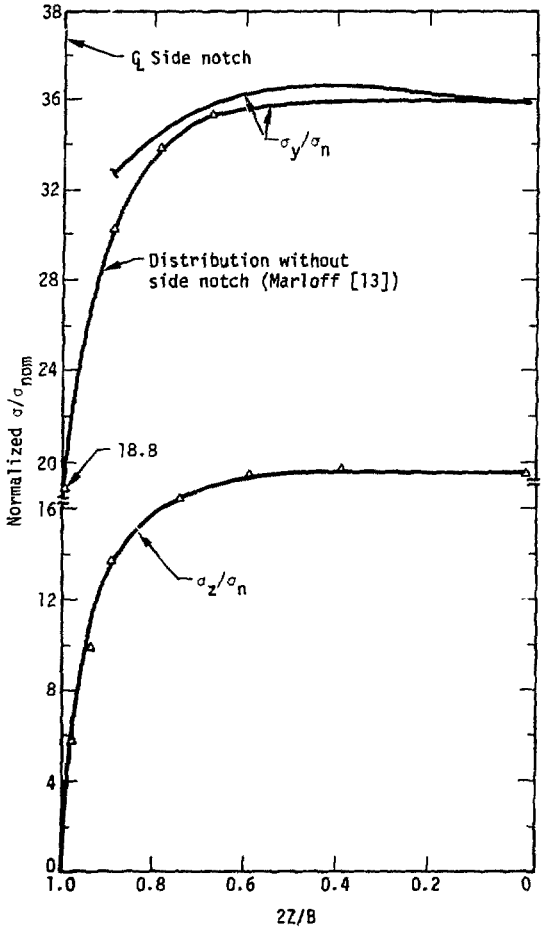

Kirkwood - Fig. 8

F8

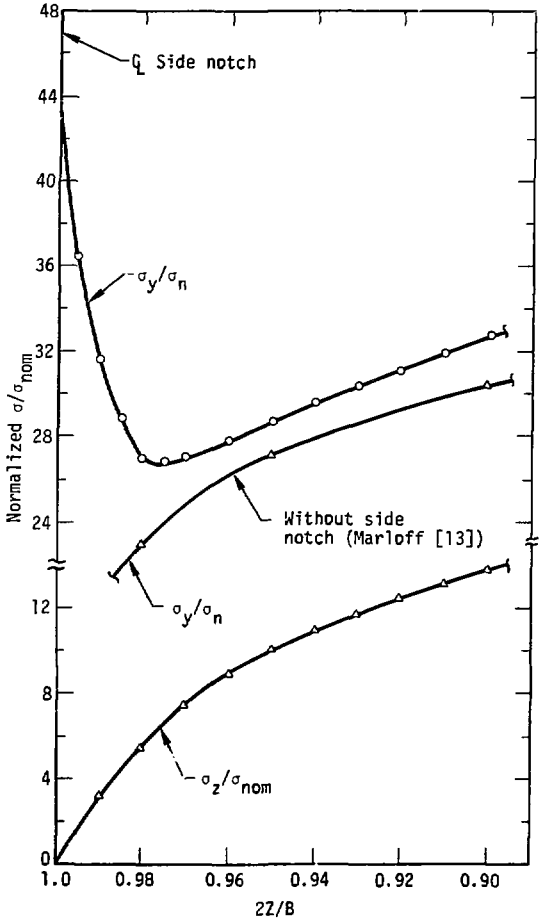

Kirkwood - Fig. 9

F9

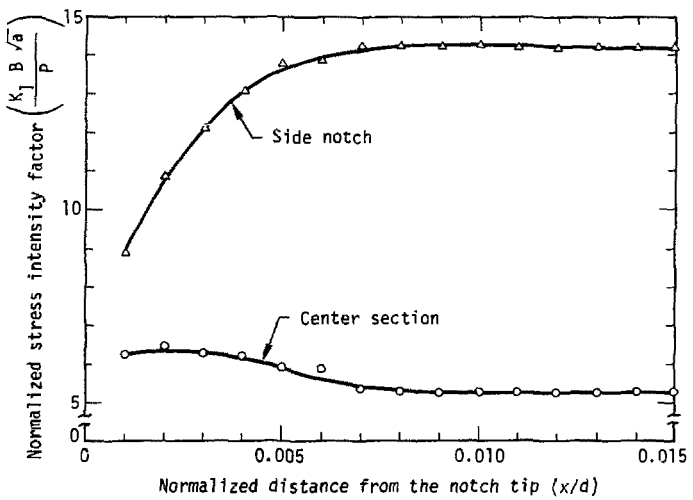

Kirkwood - Fig. 10

F1